REPORT NO. FRA-OR&D-76-09

THE EFFECT OF IMPERFECTIONS ON THE VERTICAL BUCKLING OF RAILROAD TRACKS

Yehia M. El-Aini

JUNE 1976

INTERIM REPORT

DOCUMENT IS AVAILABLE TO THE PUBLIC THROUGH THE NATIONAL TECHNICAL INFORMATION SERVICE, SPRINGFIELD, VIRGINIA 22161

Prepared for

U.S. DEPARTMENT OF TRANSPORTATION
FEDERAL RAILROAD ADMINISTRATION
Office of Research and Development
Washington DC 20590

NOTICE

This document is disseminated under the sponsorship of the Department of Transportation in the interest of information exchange. The United States Government assumes no liability for its contents or use thereof.

NOTICE

The United States Government does not endorse products or manufacturers. Trade or manufacturers' names appear herein solely because they are considered essential to the object of this report.

TECHNICAL REPORT STANDARD TITLE PAGE

1. Report No.	2. Government Accession No.	3. Recipient's Catalog No.
FRA-OR&D-76-09		

4. Title and Subtitle	5. Report Date
THE EFFECT OF IMPERFECTIONS ON THE VERTICAL BUCKLING OF RAILROAD TRACKS	June 1976
	6. Performing Organization Code

7. Author(s)	8. Performing Organization Report No.
Yehia M. El-Aini	DOT-TSC-FRA-75-17

9. Performing Organization Name and Address	10. Work Unit No.
Princeton University* School of Engineering and Applied Science Princeton NJ 08540	RR519/R6321
	11. Contract or Grant No. DOT-TSC-900
	13. Type of Report and Period Covered Interim Report January - April 1975
12. Sponsoring Agency Name and Address U.S. Department of Transportation Federal Railroad Administration Office of Research and Development Washington DC 20590	14. Sponsoring Agency Code

15. Supplementary Notes
*Under contract to: U.S. Department of Transportation
Transportation Systems Center
Kendall Square
Cambridge MA 02142

16. Abstract

This report deals with an analytic prediction of the effect of geometric imperfections on the post-buckling characteristics of railroad tracks. The analysis is restricted to the case of vertical track buckling due to constrained thermal expansion in which the track is assumed to lift itself up over a finite span. The imperfections are categorized into two cases: Case (A) in which the region of imperfection is larger than the span of lift-off and Case (B) in which the imperfection region is smaller than the span of lift-off. It is shown that while a perfectly straight track does not exhibit bifurcation points from the undeformed state, the imperfect track does and that the bifurcation temperature in Case (A) is lower than in Case (B) for the same ratio of imperfection amplitudes reduces the bifurcation temperatures significantly. It is found that the bifurcation temperature as well as the safe temperature increase are higher for heavier tracks.

17. Key Words	18. Distribution Statement
Vertical Buckling Imperfect Tracks Thermal Buckling Track Stability	DOCUMENT IS AVAILABLE TO THE PUBLIC THROUGH THE NATIONAL TECHNICAL INFORMATION SERVICE, SPRINGFIELD, VIRGINIA 22161

19. Security Classif. (of this report)	20. Security Classif. (of this page)	21. No. of Pages	22. Price
Unclassified	Unclassified	40	

Form DOT F 1700.7 (8-69)

PREFACE

This report has been prepared by Princeton University as part of the Improved Track Structure Research Program managed by the Transportation Systems Center (TSC). This program was sponsored by the Office of Research and Development, Improved Track Structure Research Division, of the Federal Railroad Administration, Washington DC 20590.

The report presents the results of a study dealing with analytically predicting the effect of geometric imperfections on the buckling of railroad track in the vertical plane, when subjected to uniform thermal expansions.

Dr. Andrew Kish, at the Transportation Systems Center, Cambridge, Mass. was the technical monitor for the work under this contract, and his cooperation and suggestions are gratefully acknowledged. The guidance and useful comments provided by Professor Arnold D. Kerr of Princeton University during the course of this investigation are deeply appreciated.

METRIC CONVERSION FACTORS

Approximate Conversions to Metric Measures

Symbol	When You Know	Multiply by	To Find	Symbol
		LENGTH		
in	inches	2.5	centimeters	cm
ft	feet	30	centimeters	cm
yd	yards	0.9	meters	m
mi	miles	1.6	kilometers	km
		AREA		
in^2	square inches	6.5	square centimeters	cm^2
ft^2	square feet	0.09	square meters	m^2
yd^2	square yards	0.8	square meters	m^2
mi^2	square miles	2.6	square kilometers	km^2
	acres	0.4	hectares	ha
		MASS (weight)		
oz	ounces	28	grams	g
lb	pounds	0.45	kilograms	kg
	short tons (2000 lb)	0.9	tonnes	t
		VOLUME		
tsp	teaspoons	5	milliliters	ml
Tbsp	tablespoons	15	milliliters	ml
fl oz	fluid ounces	30	milliliters	ml
c	cups	0.24	liters	l
pt	pints	0.47	liters	l
qt	quarts	0.95	liters	l
gal	gallons	3.8	liters	l
ft^3	cubic feet	0.03	cubic meters	m^3
yd^3	cubic yards	0.76	cubic meters	m^3
		TEMPERATURE (exact)		
°F	Fahrenheit temperature	5/9 (after subtracting 32)	Celsius temperature	°C

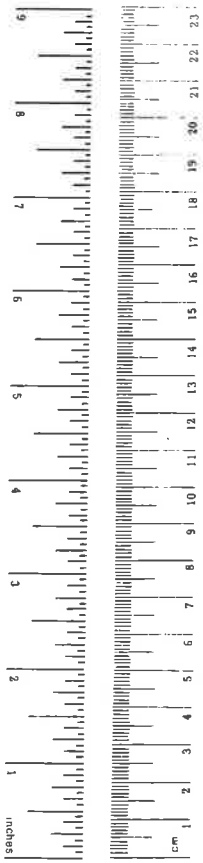

Approximate Conversions from Metric Measures

Symbol	When You Know	Multiply by	To Find	Symbol
		LENGTH		
mm	millimeters	0.04	inches	in
cm	centimeters	0.4	inches	in
m	meters	3.3	feet	ft
m	meters	1.1	yards	yd
km	kilometers	0.6	miles	mi
		AREA		
cm^2	square centimeters	0.16	square inches	in^2
m^2	square meters	1.2	square yards	yd^2
km^2	square kilometers	0.4	square miles	mi^2
ha	hectares (10,000 m^2)	2.5	acres	
		MASS (weight)		
g	grams	0.035	ounces	oz
kg	kilograms	2.2	pounds	lb
t	tonnes (1000 kg)	1.1	short tons	
		VOLUME		
ml	milliliters	0.03	fluid ounces	fl oz
l	liters	2.1	pints	pt
l	liters	1.06	quarts	qt
l	liters	0.26	gallons	gal
m^3	cubic meters	35	cubic feet	ft^3
m^3	cubic meters	1.3	cubic yards	yd^3
		TEMPERATURE (exact)		
°C	Celsius temperature	9/5 (then add 32)	Fahrenheit temperature	°F

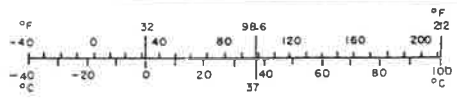

CONTENTS

ILLUSTRATIONS

1. INTRODUCTION

In a recent survey of the literature on vertical track buckling, A. D. Kerr [1]* discussed the various aspects of the problem indicating that the use of linearized analyses may lead to incorrect results. Then it was shown by Kerr and El-Aini in [2] and by El-Aini in [3] that for the problem of vertical track buckling, due to constrained thermal expansion, the response of a quasi-linear formulation is very close to that of a formulation with higher non-linearities.

In both references [2] and [3], the track was assumed to be perfectly straight. The fact that an actual track may encounter different types of geometric imperfections makes it necessary to examine the effect of these imperfections on the post-buckling response of the track structure.

In 1973, Kerr [4] showed on a model, which exhibits the characteristic features of a track in the vertical plan, that the presence of initial imperfections reduces the range of safe-temperature increase.

In view of the above findings and because of the potential importance of the obtained results in railroad mechanics, it seemed necessary to solve the problem of vertical track buckling with geometric imperfections, which is the subject of this report.

For mathematical convenience, geometric imperfections may be classified into two main categories: (A) the imperfection region is larger than the span of lift-off and (B) the imperfection region is smaller than the lift-off span, as shown in Figure 1.

In the following analysis, the problem is formulated using a variational approach to ensure mathematically consistent differential equations, boundary conditions and matching conditions [5].

*Numbers in brackets denote references

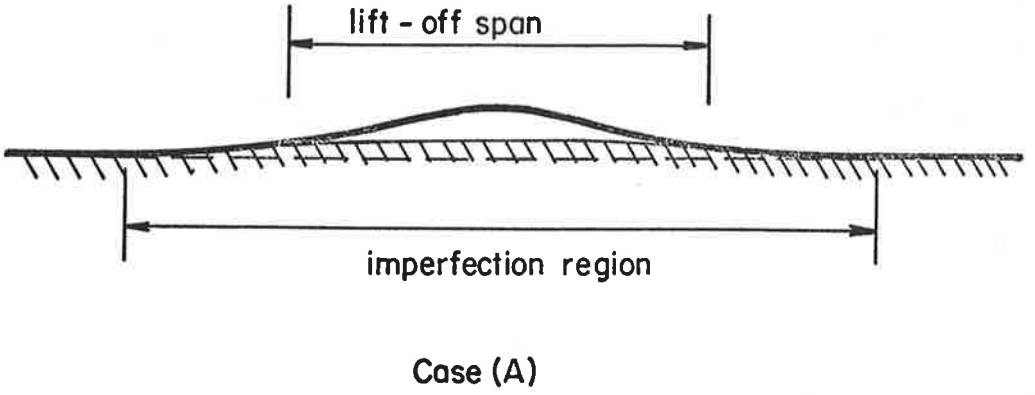

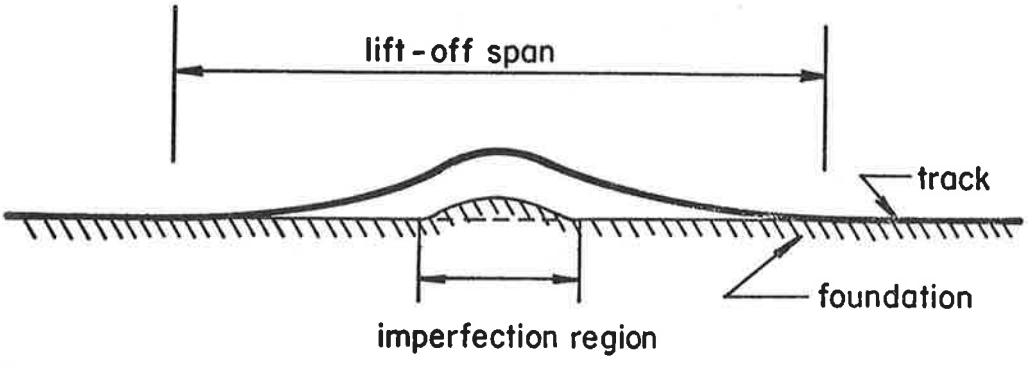

FIGURE 1. BUCKLED CONFIGURATIONS IN CASES (A) AND (B)

The results are presented for "light" and "heavy" tracks. The first corresponds to a track with wood cross ties and 57 kg/m rails (115 lb/yard) and the second corresponds to a track with concrete cross ties and 68 kg/m rails (136 lb/yard).

2. FORMULATION OF THE PROBLEM

In the following analysis, the track will be idealized by an equivalent infinite beam of uniform cross section resting on a rigid foundation. The following additional assumptions are made:

1) The beam is subject to a uniform-temperature increase of magnitude T. This increase is measured from the neutral laying temperature of the track. In addition a uniformly distributed weight of intensity q is assumed to be acting along the reference axis of the beam.

2) The beam is assumed to undergo deformations in the x-z plane only, which are symmetric with respect to the origin (x = 0).

3) The deformed configuration is assumed to consist of two regions: a lift-off region, $-a \leq x \leq a$, and an attached outer region.

4) The foundation resistance, to the axial displacements of the beam elements, is represented by a series of linear springs with stiffness coefficient k_h (Winkler model), acting at the center line of the beam and throughout the attached region [2].

5) The initial imperfect state is stressless.

6) The beam is made of homogeneous, isotropic and linearly elastic material with modulus of elasticity E.

With the above assumptions, two types of geometric imperfections will be discussed in the following section.

2.1 CASE (A): THE IMPERFECTION REGION IS LARGER THAN THE SPAN OF LIFT-OFF

In this case, the initial imperfected shape is assumed to be of the form

$$w_o(x) = \begin{cases} -\frac{f}{2}\left[1 + \cos\frac{\pi x}{\ell}\right]; \quad -\ell \leq x \leq \ell & ; \quad \ell > a \\ 0 & ; \text{ elsewhere} \end{cases}$$

and

$$u_o(x) = 0 \quad ; \qquad -\infty \leq x \leq \infty \tag{1}$$

The deformed equilibrium configuration for this case is schematically presented in Figure 2.

Assuming the validity of the plane section hypothesis and using the theory of Ref. [6], it follows that

$$\varepsilon_{xx} = (\hat{u}_{,x} + \frac{1}{2}\hat{w}^2_{,x} - z\hat{w}_{,xx}) - \alpha T \tag{2}$$

where $(\ )_{,x} = d(\ )/dx$ and α is the coefficient of thermal expansion. The $(\hat{})$ terms refers to the deformations of the reference x-axis.

Denoting the lift-off region by (1) and the attached region by (2), it follows that

$$\begin{aligned} u_1^* &= \hat{u}_1 + u_o \quad ; \quad u_2^* = \hat{u}_2 + u_o \\ w_1^* &= \hat{w}_1 + w_o \quad ; \quad w_2^* = \hat{w}_2 + w_o \end{aligned} \tag{3}$$

where the star denotes the total deflections.

Substituting (3) into (2) it follows that

$$\varepsilon^*_{ixx} = \varepsilon_{oxx} + \tilde{\varepsilon}_{ixx} \quad ; \quad i = 1, 2 \tag{4}$$

where

$$\varepsilon_{oxx} = (u_{o,x} + \frac{1}{2} w_{o,x}^2) - z w_{o,xx} \tag{5}$$

CASE (A)

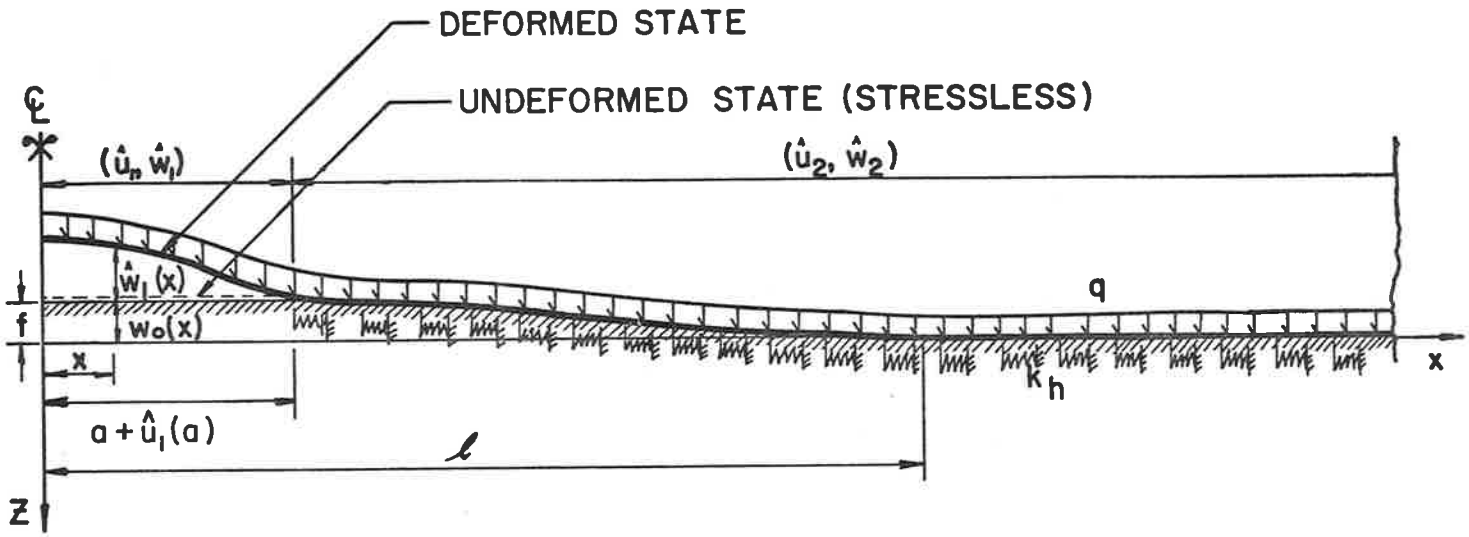

FIGURE 2. MATHEMATICAL MODEL FOR CASE (A)

and

$$\tilde{\varepsilon}_{ixx} = (\hat{\varepsilon}_{ixx} - z\hat{w}_{i,xx}) - \alpha T \qquad 6)$$

and

$$\hat{\varepsilon}_{ixx} = \hat{u}_{i,x} + \frac{1}{2}\hat{w}_{i,x}^2 + \hat{w}_{i,x}w_{o,x} \qquad 7)$$

Since the initial state is stress free, Hooke's law may be written as

$$\sigma_{ixx} = E\tilde{\varepsilon}_{ixx} \qquad 8)$$

Utilizing the principle of stationary total potential energy, the differential equations of equilibrium together with the boundary conditions are derived from the condition

$$\delta\Pi = 0 \qquad 9)$$

where

$$\Pi = (U - W) \qquad 10)$$

and

U = the elastic strain energy of the system

and

W = the work potential of the surface and body forces.

Because of the assumed symmetry of deformations, U and W may be written as:

$$\left.\begin{aligned} U &= 2\int_0^a \left(\iint_A \frac{1}{2}E\tilde{\varepsilon}_{1xx}^2\, dA\right)dx + 2\int_a^\infty \left(\iint_A \frac{1}{2}E\tilde{\varepsilon}_{2xx}^2\, dA\right)dx + 2\int_a^\infty \frac{1}{2}k_h\hat{u}_2^2 dx \\ \text{and}\quad W &= 2\int_0^a q\hat{w}_1\, dx + 2\int_a^\infty q\hat{w}_2\, dx \end{aligned}\right\} \qquad 11)$$

Because of the constraint that $\hat{w}_2$ together with all its higher derivatives have to be identically zero, a number of Lagrange multipliers have to be used to insure a mathematically consistent formulation.

Let

$$\Pi^* = \Pi + 2\int_a^\infty \lambda_1 \hat{w}_2 dx + 2\lambda_2 \hat{w}_2(a) + 2\lambda_3 \hat{w}_2'(a) \quad , \tag{12}$$

where λ_1, λ_2 and λ_3 are Lagrange multipliers. Now the D.E.'s* and B.C.'s* are obtained from

$$\delta\Pi^* = 0 \tag{13}$$

Performing the integration over the area, it follows that

$$\Pi^* = \int_0^a F_1 dx + \int_a^\infty F_2 dx + 2\lambda_2 \hat{w}_2(a) + 2\lambda_3 \hat{w}_2'(a) \quad , \tag{14}$$

where

$$F_1 = EA(\hat{\varepsilon}_{1xx} - \alpha T)^2 + EI\hat{w}_{1,xx}^2 - 2q\hat{w}_1 \tag{15}$$

$$F_2 = EA(\hat{\varepsilon}_{2xx} - \alpha T)^2 + EI\hat{w}_{2,xx}^2 + k_h \hat{u}_2^2 - 2q\hat{w}_2 + 2\lambda_1 \hat{w}_2 \quad . \tag{16}$$

Noting that a is a variable end point, the first variation of Π^*, following [7], is

$$\delta\Pi^* = \delta \int_0^a F_1 dx + \delta \int_a^\infty F_2 dx + (F_1 - F_2)\Big|_{x=a} \delta a + 2\lambda_2 \delta\hat{w}_2\Big|_{x=a}$$

$$+ 2\lambda_3 \delta\hat{w}_2'\Big|_{x=a} \quad . \tag{17}$$

*Denote differential equation and boundary conditions respectively.

Conducting the variations in (17), it follows that

$$\frac{1}{2}\delta\Pi^* = \int_0^a \left\{-[(EA\varepsilon_1)_{,x}]\delta\hat{u}_1 + [(EI\hat{w}_{1,xx})_{,xx} - [EA\varepsilon_1(w_{0,x} + w_{1,x})]_{,x} - q]\delta\hat{w}_1\right\} dx$$

$$+ \int_a^\infty \left\{[-(EA\varepsilon_1)_{,x} + k_h\hat{u}_2]\delta\hat{u}_2 + [(EI\hat{w}_{2,xx})_{,xx} - [EA\varepsilon_2(w_{0,x} + w_{2,x})]_{,x} - q + \lambda_1]\delta\hat{w}_2\right\} d$$

$$+ \left\{-[EA\varepsilon_1]\delta\hat{u}_1 - [EA\varepsilon_1\hat{w}_{1,x} - (EI\hat{w}_{1,xx})_{,x}]\delta\hat{w}_1 - [EI\hat{w}_{1,xx}]\delta\hat{w}_{1,x}\right\}_{x=0}$$

$$+ \left\{\frac{1}{2}(F_1 - F_2)\delta a + [EA\varepsilon_1\delta\hat{u}_1 - EA\varepsilon_2\delta\hat{u}_2] + [EA\varepsilon_1\hat{w}_{1,x} - (EI\hat{w}_{1,xx})_{,x}]\delta\hat{w}_1\right.$$

$$- [EA\varepsilon_2\hat{w}_{2,x} - (EI\hat{w}_{2,xx})_{,x} - \lambda_2]\delta\hat{w}_2 + (EI\hat{w}_{1,xx})\delta\hat{w}_{1,x}$$

$$\left. - [EIw_{2,xx} - \lambda_3]\delta w_{2,x}\right\}_{x=a} + \left\{(EA\varepsilon_2)\delta\hat{u}_2 + \right.$$

$$\left.[EA\varepsilon_2\hat{w}_{2,x} - (EI\hat{w}_{2,xx})_{,x}]\delta\hat{w}_2 + [EI\hat{w}_{2,xx}]\delta\hat{w}_{2,x}\right\}_{x=\infty} = 0 \quad , \qquad 18)$$

where

$$\varepsilon_i = \hat{\varepsilon}_{ixx} - \alpha T, \quad i = 1.2 \quad .$$

Since a is a variable endpoint, the variations of the functions $\hat{u}_1$, $\hat{u}_2$, $\hat{w}_1$, $\hat{w}_2$, $\hat{w}_{1,x}$ and $\hat{w}_{2,x}$ at x = a are interrelated in the manner described in [2] and [3], as follows:

$$\delta\eta_i(a) = \delta\eta - \eta_{i,x}(a)\delta a, \quad i = 1, 2 \quad , \qquad 19)$$

and $\eta_i(x)$ stands for any of the above-mentioned functions.

Applying the fundamental lemma of calculus of variations and noting the continuity of the beam at the separation point, the D. E.'s are:

$$\left.\begin{aligned} EI\hat{w}_{1,xxxx} - [EA(\hat{\varepsilon}_{1xx} - \alpha T)(w_{o,x} + \hat{w}_{1,x})]_{,x} &= q \\ -[EA(\hat{\varepsilon}_{1xx} - \alpha T)]_{,x} &= 0 \end{aligned}\right\} \quad 0 \leq x \leq a \quad , \qquad \begin{aligned} &20.a) \\ &20.b) \end{aligned}$$

and

$$\left.\begin{aligned} EI\hat{w}_{2,xxxx} - [EA(\hat{\varepsilon}_{2xx} - \alpha T)(w_{o,x} + \hat{w}_{2,x})]_{,x} &= (q - \lambda_1) \\ -[EA(\hat{\varepsilon}_{2xx} - \alpha T)] + k_h \hat{u}_2 &= 0 \\ \hat{w}_2(x) \equiv \hat{w}_{2,x}(x) \equiv \hat{w}_{2,xx} \equiv \cdots &\equiv 0 \end{aligned}\right\} \quad a \leq x \leq \infty \quad . \qquad \begin{aligned} &21.a) \\ &21.b) \\ &21.c) \end{aligned}$$

The boundary and transversality conditions reduce to:*

<u>at x = 0</u>:

$$\hat{u}_1(0) = 0 \qquad 22.a)$$

$$\hat{w}_{1,x}(0) = 0 \qquad 22.b)$$

$$\hat{w}_{1,xxx}(0) = 0 \quad , \qquad 22.c)$$

<u>at x = a</u>:

$$\hat{w}_1(a) = \hat{w}_2(a) \qquad 22.d)$$

$$\hat{w}_{1,x}(a) = \hat{w}_{2,x}(a) \qquad 22.e)$$

$$EI\hat{w}_{1,xx}(a) = EI\hat{w}_{2,xx}(a) - \lambda_3 \qquad 22.f)$$

$$-EI\hat{w}_{1,xxx}(a) = -EI\hat{w}_{2,xxx}(a) - \lambda_2 \qquad 22.g)$$

$$\hat{u}_1(a) = \hat{u}_2(a) \qquad 22.h)$$

$$EA\hat{\varepsilon}_{1xx}(a) = EA\hat{\varepsilon}_{2xx}(a) \quad , \qquad 22.i)$$

and

$$\text{T. C.}^{**} \qquad \hat{w}_{1,xx}(a) = \hat{w}_{2,xx}(a) \quad , \qquad 22.j)$$

---

* For details and comments on the difficulties encountered with the discontinuities of the Winkler model, at the separation point, refer to [2].

** T. C. denotes transversality condition.

at $x = \infty$,

$$\text{(k)} \quad \hat{u}_2(\infty) = 0 \tag{22.k}$$

$$\hat{w}_2(\infty) = 0 \tag{22.l}$$

$$\text{(m)} \quad \hat{w}_{2,x}(\infty) = 0 \quad . \tag{22.m}$$

From T. C. (22) (j) and B. C. (22) (f), it follows that

$$\lambda_3 = 0 \quad , \tag{23}$$

which implies the continuity of bending moments at the separation point, while B. C. (22)(g) indicates a discontinuity of the shearing forces at $x = a$. This is attributed to the neglection of the shear deformation in the strain energy expression.

2.2 ANALYTICAL SOLUTION OF CASE (A)

Integrating (20.b) once it follows that

$$-EA(\hat{\varepsilon}_{1xx} - \alpha T) = \text{Const.} = N \quad . \tag{24}$$

Substitution of (24) into D. E. (20.a), it becomes

$$\hat{w}_{1,xxxx} + \kappa^2 \hat{w}_{1,xx} = q^* - \kappa^2 w_{o,xx} \quad , \tag{25}$$

where

$$\kappa^2 = N/EI; \; q^* = q/EI \quad . \tag{26}$$

Utilizing the expression for $w_0(x)$ in (1), the general solution to D. E. (25) takes the form

$$\hat{w}_1(x) = A_1 + A_2 x + A_3 \cos \kappa x + A_4 \sin \kappa x + \frac{q^*}{2\kappa^2} x - \rho \cos\left(\frac{\pi x}{\ell}\right) , \tag{27}$$

where A_1, A_2, A_3 and A_4 are constants and

$$\rho = \frac{\kappa^2 f}{2[(\pi/\ell)^2 - \kappa^2]} \qquad 28)$$

Because of symmetry around the origin, it follows that

$$A_2 \equiv A_4 \equiv 0 \quad , \qquad 29)$$

and the general solution reduces to

$$\hat{w}_1(x) = A_1 + A_3 \cos\kappa x + \frac{q^*}{2\kappa^2} x^2 - \rho \cos\frac{\pi x}{\ell} \qquad 30)$$

Substitution of equations (30) and (21.c) into B.C.'s (22)(d) and (22)(e), it follows that

$$A_3 = [\frac{q^* a}{\kappa^2} + \frac{\rho\pi}{\ell} \sin(\frac{\pi a}{\ell})]/\kappa \sin\kappa a \quad , \qquad 31)$$

and

$$A_1 = - A_3 \cos\kappa a - \frac{q^* a^2}{2\kappa^2} + \rho \cos(\frac{\pi a}{\ell}) \qquad 32)$$

Substitution of (31) and (32) into (30), it follows that

$$\hat{w}_1(x) = \left[\frac{\frac{q^* a}{\kappa^2} + \frac{\rho\pi}{\ell} \sin\frac{\pi a}{\ell}}{\kappa \sin\kappa a}\right](\cos\kappa x - \cos\kappa a) +$$

$$\frac{q^*}{2\kappa^2}(x^2 - a^2) - \rho(\cos\frac{\pi x}{\ell} - \cos\frac{\pi a}{\ell}) \; ; \; 0 \leqq x \leqq a;$$

$$\ell > a \, . \qquad 33)$$

The transversality condition (22)(j) gives an additional equation to determine the unknown a for any given value of κ, namely:

$$- \frac{[\frac{q^* a}{\kappa} + \kappa \frac{\rho\pi}{\ell} \sin\frac{\pi a}{\ell}]}{\tan\kappa a} + \frac{q^*}{\kappa^2} + \rho(\frac{\pi}{\ell})^2 \cos\frac{\pi a}{\ell} = 0 \quad . \qquad 34)$$

In the limit if $f \to 0$, (34) reduces to

$$\tan \kappa a = \kappa a \qquad 35)$$

which is the transversality condition for the case without imperfection.

The solution for the axial displacement in the lift-off region is obtained as follows:

Equation (20.b) may be written as

$$\hat{u}_{1,x}(x) = [-\frac{N}{EA} + \alpha T - \frac{1}{2}\hat{w}^2_{1,x} - \hat{w}_{1,x}w_{o,x}] \quad . \qquad 36)$$

Integrating (36) once and noting B. C. (22)(a), it follows that

$$\hat{u}_1(x) = (-\frac{N}{EA} + \alpha T)x - \int_0^{x} (\frac{1}{2} w^2_{1,\xi} + \hat{w}_{1,\xi}w_{o,\xi})d\xi \quad . \qquad 37)$$

Considering D. E. (21.b) and noting equations (8) and (21.c), it reduces to

$$\hat{u}_{2,xx} - \beta^2\hat{u}_2 = 0 \quad , \qquad 38)$$

where

$$\beta^2 = (k_h/EA) \quad . \qquad 39)$$

The general solution of D. E. (38) is

$$\hat{u}_2(x) = C_1 e^{-\beta x} + C_2 e^{+\beta x} \quad . \qquad 40)$$

Because of the regularity condition (22)(k) at ∞, it follows that

$$C_2 \equiv 0 \quad ,$$

hence,

$$\hat{u}_2(x) = c_1 e^{-\beta x} \quad . \qquad 41)$$

B. C. (22)(i) reduces to

$$\hat{u}_{1,x}(a) = \hat{u}_{2,x}(a) \quad . \tag{42}$$

Substitution of (36) and (41) into (42) gives

$$C_1 = \frac{e^{\beta a}}{-\beta}\left[-\frac{N}{EA} + \alpha T\right] \quad , \tag{43}$$

and the solution to $\hat{u}_2(x)$ becomes

$$\hat{u}_2(x) = \frac{e^{-\beta(x-a)}}{-\beta}\left[-\frac{N}{EA} + \alpha T\right] \quad . \tag{44}$$

Now, substitution of (44) and (37) into B. C. (22)(h) gives

$$T = \left\{\left(\frac{N}{EA}\right) + \frac{1}{\left(1 + \frac{1}{\beta a}\right)} \frac{1}{a} \int_0^a \left(\frac{1}{2}\hat{w}_{1,x} + \hat{w}_{1,x} w_{o,x}\right) dx\right\} / \alpha \quad , \tag{45}$$

which is the temperature increase corresponding to a state of lift-off over a span 2a.

The process of evaluating the post-buckling response may be summarized as follows:

1) For a chosen value of the axial load N, (34) is solved iteratively through a Newton-Raphson scheme to determine the corresponding value of a.

2) Knowing N and a, the solution for $\hat{w}_1(x)$ is determined and the integrals in (45) can be evaluated in closed form.

3) The use of (45) gives the temperature increase corresponding to the equilibrium state $\hat{w}_1(x)$.

Typical values of the track parameters are listed in Table 1. They correspond to a track with wood ties (light track) and a track with concrete ties (heavy track).

TABLE 1 TYPICAL VALUES OF TRACK PARAMETERS

Track Parameter	Light track		Heavy track	
Weight of rail, [8]	57	kg / m(115 lb/yd)	68	kg / m(136 lb/yd)
Weight of track structure (q) *	315	kg / m	680	kg/m
Cross-sectional area of two rails (A)	0.0145	m^2	0.0172	m^2
Moment of inertia of two rails (I)	5.47×10^{-5}	m^4	8.0×10^{-5}	m^4
Axial resistance of the foundation (k_h) (estimate)	5×10^4	kg / m/m	5×10^4	kg/m/m
Modulus of elasticity (E) of rails	2.1×10^{10}	kg/m^2	2.1×10^{10}	kg / m^2
Coefficient of thermal expansion	10.5×10^{-6}		10.5×10^{-6}	

To demonstrate the basic features of the solution, the results for an example problem are shown in Figures 3, 4, 5 and 6. For this particular example the imperfection span, 2ℓ, is chosen to be 100 meters, while the imperfection amplitude f is varied from 0.0 to 1.0 meter.

Figure 3 shows the equilibrium branches for different values of f. For each value of f, the response consists of two branches. The first branch is vertical and corresponds to the pre-buckling state. The second branch bifurcates from the vertical one† and shows a minimum below which the only state of equilibrium is the undeformed state. It may be shown, using the Lagrange stability criteria, that the vertical branch is stable while the second branch is unstable between the bifurcation point and the point of minimum and is stable elsewhere [4]. The temperature increase corresponding to the point of minimum is referred to as the "safe" temperature increase.

*Weight is estimated for a track with the following characteristics: 3250 ties, 6500 tieplates, 13,000 spikes, 4500 anchors/mile [9].

†Except for f = 0.0.

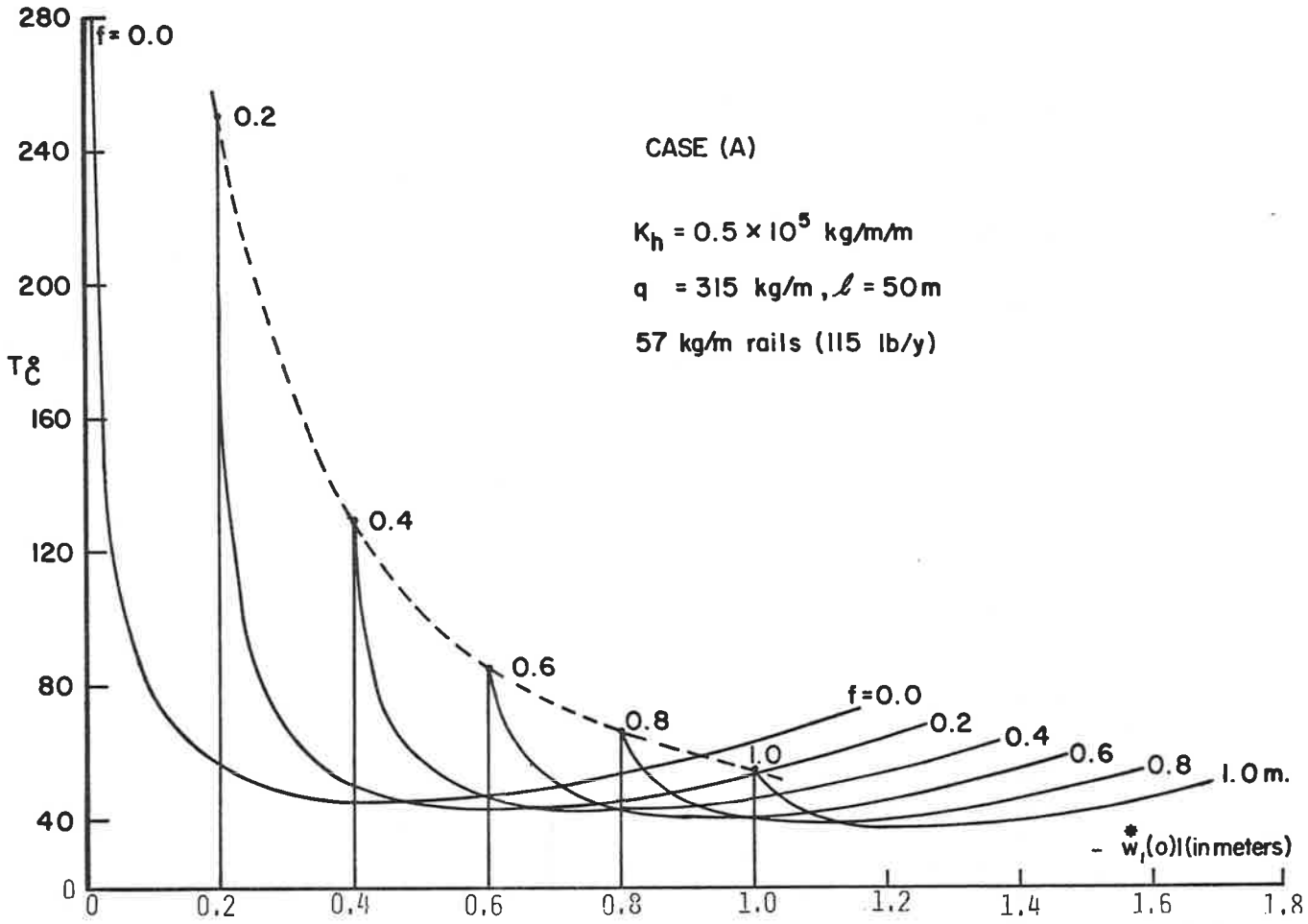

FIGURE 3. TEMPERATURE INCREASE VS. MAXIMUM DEFLECTION FOR CASE (A) (LIGHT TRACK)

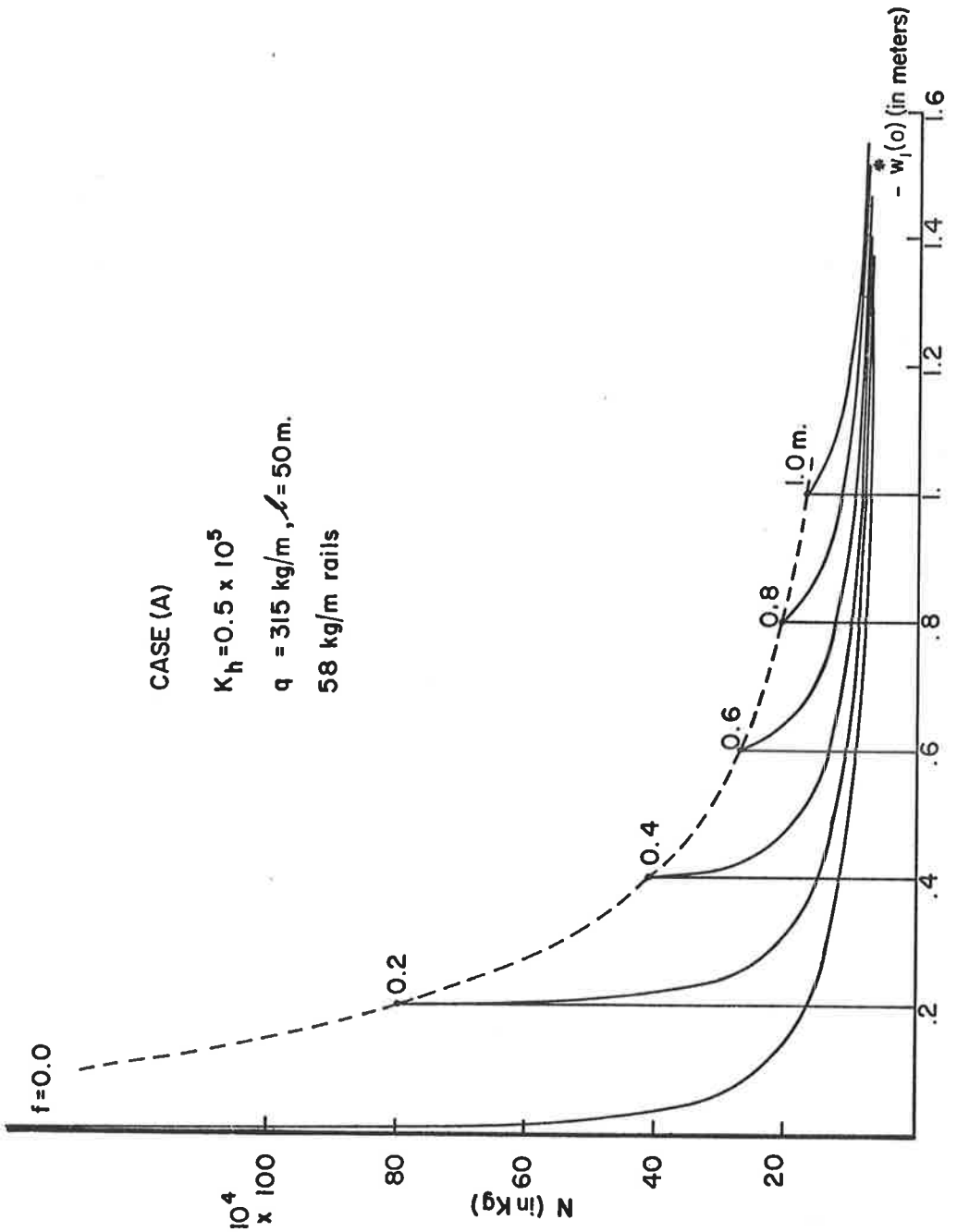

FIGURE 4. AXIAL LOAD IN BUCKLED REGION VS. MAXIMUM DEFLECTION FOR CASE (A) (LIGHT TRACK)

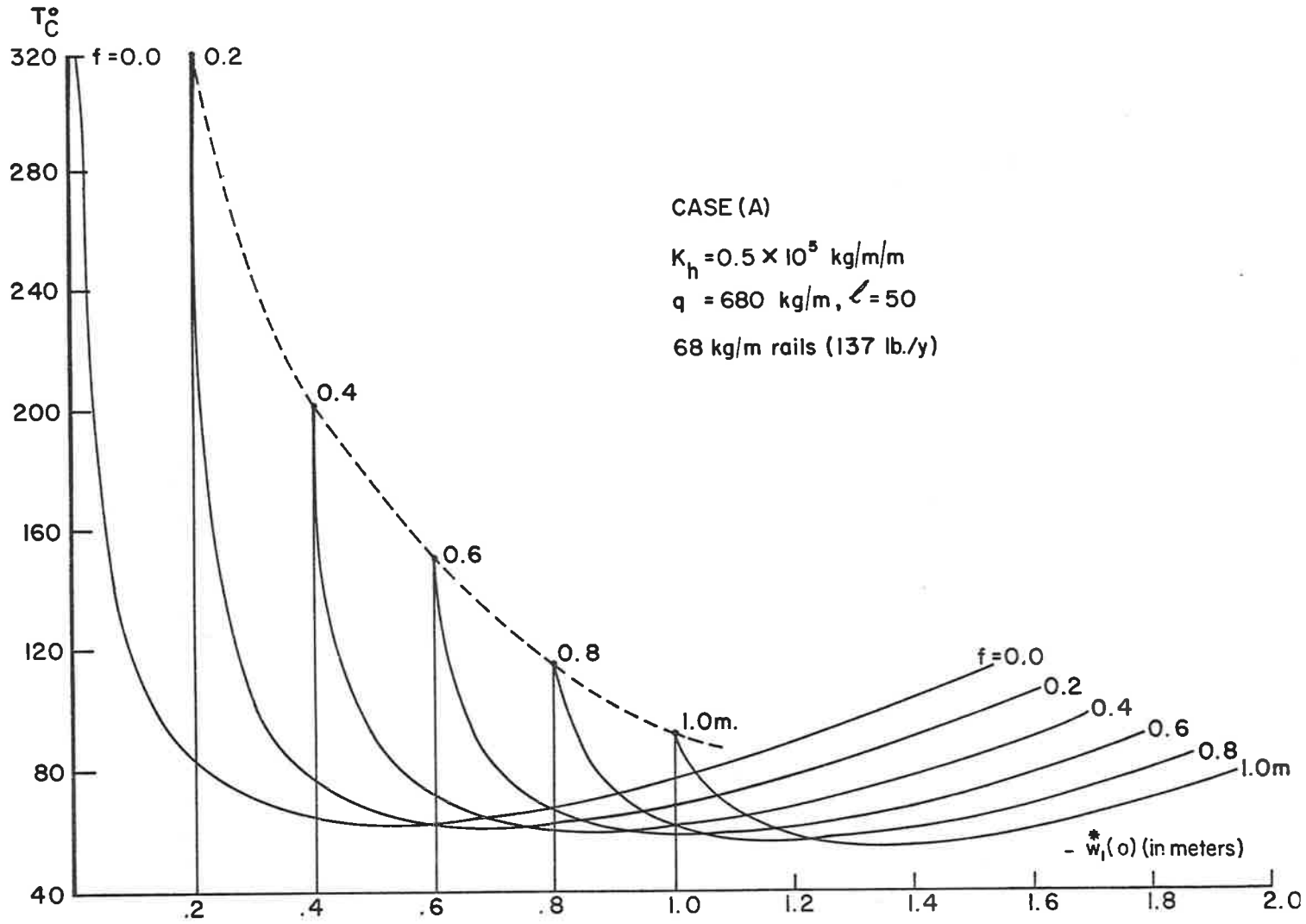

FIGURE 5. TEMPERATURE INCREASE VS. MAXIMUM DEFLECTION FOR CASE (A) (HEAVY TRACK)

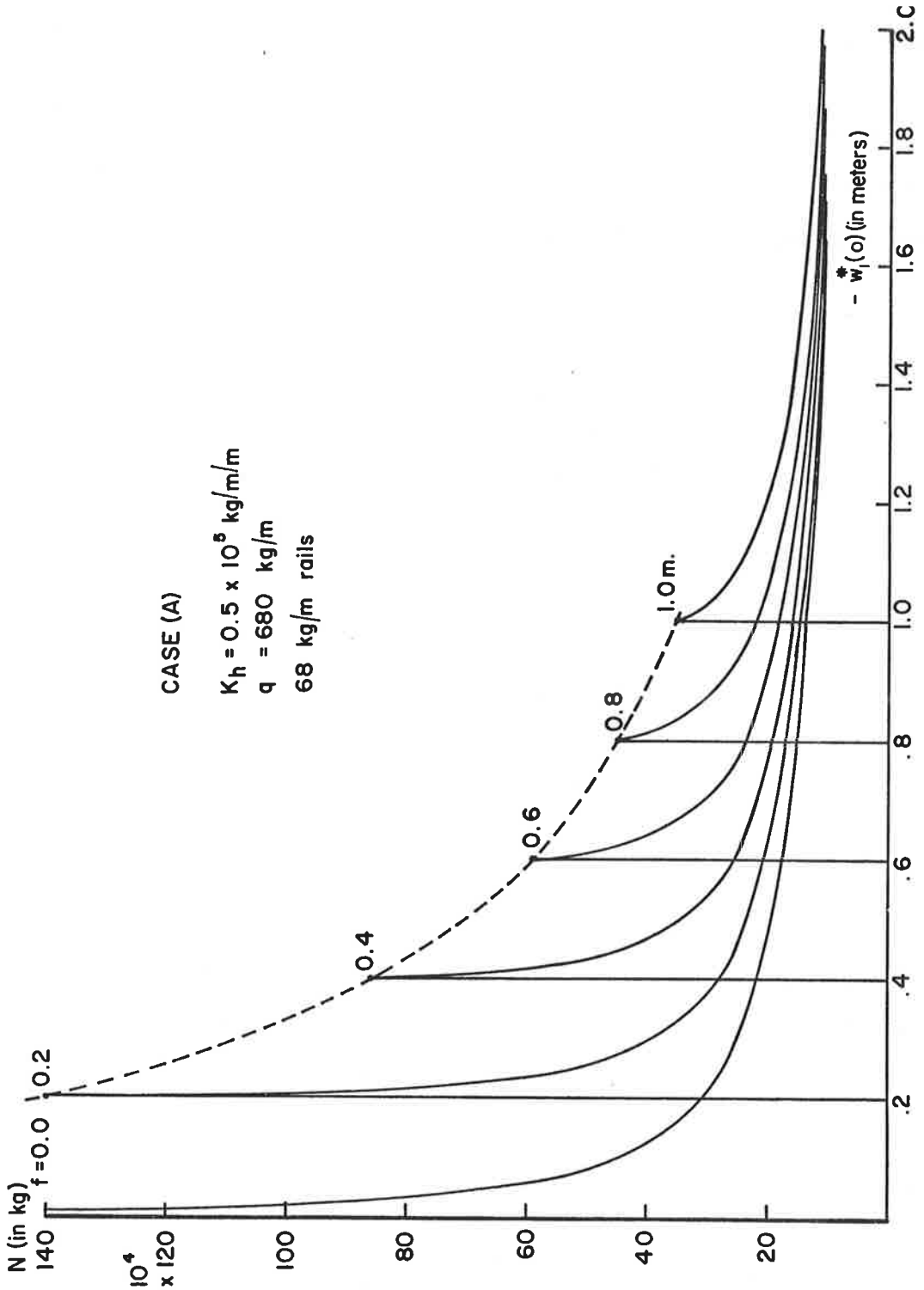

FIGURE 6. AXIAL LOAD IN BUCKLED REGION VS. MAXIMUM DEFLECTION FOR CASE (A) (HEAVY TRACK)

Increasing the amplitude of imperfection from 0.0 to 1.0 reduces slightly the critical temperature from 45° to 37°C, while the drop in the bifurcation temperature is extremely sharp. It drops from ∞ for f = 0 to 54°C for f = 1.0.

In Figure 4, the relation between the axial load and the maximum displacement is shown. The bifurcation loads are related to the bifurcation temperatures in Figure 3, through the relation

$$N_b = EA\alpha T_b \qquad 46)$$

where the subscript b denotes the bifurcation point.

It is thus obvious that increasing the imperfection amplitude will sharply reduce the bifurcation loads. For small values of the imperfection, the bifurcation loads may be higher than the yield loads for the rails;* however, buckling may still occur at temperatures much lower than the bifurcation temperatures by giving the track a disturbance large enough to put it on the unstable part of the equilibrium branch. These disturbances may be encountered during the maintenance process or due to waves produced by the moving trains.

A similar set of graphs, figures 5 and 6, are presented for the case of the track with concrete ties. The critical temperature increase is higher than those of the track with wood ties. It may be as high as 62°C for the straight track and 53°C for an imperfection of 1.0 meter. The bifurcation temperatures are also much higher in this case, so are the corresponding bifurcation loads.

It thus may be that for the case of a heavy track with concrete ties, the chance of buckling is much lower than in the case of a light track.

---

* For a rail of yield stress 4,900 kg/cm^2 (70,000 psi), the necessary increase in temperature to cause yielding is 223°C, and the corresponding axial load (in two 57 kg/m rails) is 71 x 10^4 kg.

2.3 CASE (B): THE IMPERFECTION REGION IS SMALLER THAN THE LIFT-OFF REGION

In this case, the geometric imperfection is assumed to be in the same form as in Case (A); but on a small span such that the span of lift-off is larger than the span of imperfection; i.e.,

$$\text{and} \qquad w_0(x) = \begin{cases} -\frac{f}{2}\left[1 + \cos\frac{\pi x}{\ell}\right]; & -\ell \leq x \leq \ell \quad ; \quad \ell < a \\ 0 \quad ; & \text{elsewhere} \end{cases} \qquad 47)$$

$$u_0(x) = 0 \quad ; \quad -\infty \leq x \leq \infty \quad .$$

The deformed equilibrium configuration is shown in Figure 7.

The procedure of the derivation of the D. E.'s and B. C.'s is the same as for Case (A). The D. E.'s will take the following form:

$$\left.\begin{aligned} EI\hat{w}_{1,xxxx} - [EA(\hat{\varepsilon}_{1xx} - \alpha T)(\hat{w}_{1,x} + w_{o,x})]_{,x} &= q \qquad 48.a) \\ -[EA(\hat{\varepsilon}_{1xx} - \alpha T)]_{,x} &= 0 \qquad 48.b) \end{aligned}\right\} \quad 0 \leq x \leq \ell \,,$$

$$\left.\begin{aligned} EI\hat{w}_{2,xxxx} - [EA(\hat{\varepsilon}_{1xx} - \alpha T)w_{2,x}]_{,x} &= q \qquad 48.c) \\ -[EA(\hat{\varepsilon}_{2xx} - \alpha T)]_{,x} &= 0 \qquad 48.d) \end{aligned}\right\} \quad \ell \leq x \leq a \,,$$

and

$$\left.\begin{aligned} EI\hat{w}_{3,xxxx} - [EA(\hat{\varepsilon}_{3xx} - \alpha T)\hat{w}_{3,x}]_{,x} &= (q - \lambda_1) \qquad 48.e) \\ -[EA(\hat{\varepsilon}_{3xx} - \alpha T)]_{,x} + k_h\hat{u}_3 &= 0 \qquad 48.f) \\ \hat{w}_3(x) \equiv \hat{w}_{3,x}(x) \equiv \hat{w}_{3,xx}(x) \equiv \cdots &\equiv 0 \qquad 48.g) \end{aligned}\right\} \quad a \leq x \leq \infty \,,$$

CASE (B)

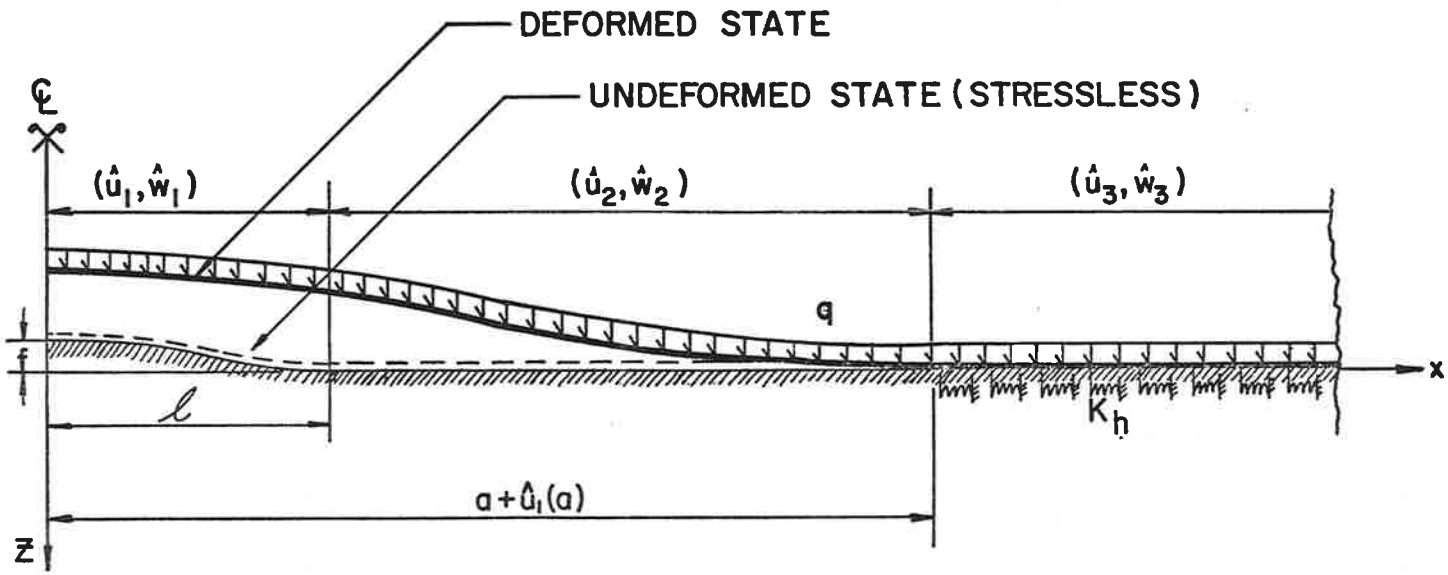

FIGURE 7. MATHEMATICAL MODEL FOR CASE (B)

The boundary and transversality conditions reduce to:

<u>at x = 0</u>:

$$\hat{u}_1(0) = 0 \qquad a)$$

$$\hat{w}_{1,x}(0) = 0 \qquad b)$$

$$\hat{w}_{1,xxx}(0) = 0 \qquad c)$$

<u>at x = ℓ</u>:

$$\hat{u}_1(\ell) = \hat{u}_2(\ell) \qquad d)$$

$$\hat{u}_{1,x}(\ell) = \hat{u}_{2,x}(\ell) \qquad e)$$

$$\hat{w}_1(\ell) = \hat{w}_2(\ell) \qquad f)$$

$$\hat{w}_{1,x}(\ell) = \hat{w}_{2,x}(\ell) \qquad g)$$

$$\hat{w}_{1,xx}(\ell) = \hat{w}_{2,xx}(\ell) \qquad h)$$

$$\hat{w}_{1,xxx}(\ell) = \hat{w}_{2,xxx}(\ell) \qquad i) \quad 49)$$

<u>at x = a</u>:

$$\hat{u}_2(a) = \hat{u}_3(a) \qquad j)$$

$$\hat{u}_{2,x}(a) = \hat{u}_{3,x}(a) \qquad k)$$

$$\hat{w}_2(a) = \hat{w}_2(a) \qquad \ell)$$

$$\hat{w}_{2,x}(a) = \hat{w}_{3,x}(a) \qquad m)$$

$$EI\hat{w}_{2,xx}(a) = EI\hat{w}_{3,xx}(a) - \lambda_3 \qquad n)$$

$$-EI\hat{w}_{2,xxx}(a) = -EI\hat{w}_{3,xxx}(a) - \lambda_2 \qquad o)$$

<u>T. C.</u>:

$$\hat{w}_{2,xx}(a) = 0 \qquad p)$$

<u>at x = ∞</u>:

$$\hat{u}_3(\infty) = 0 \qquad q)$$

$$\hat{w}_3(\infty) = 0 \qquad r)$$

$$\hat{w}_{3,x}(\infty) = 0 \; . \qquad s)$$

2.4 ANALYTICAL SOLUTION OF CASE (B)

Integrating D. E. (48.b) once, it follows that

$$-EA(\hat{\varepsilon}_{1xx} - \alpha T) = \text{const.} = N \; . \qquad 50)$$

Substitution of (50) into (48.a), it becomes

$$\hat{w}_{1,xxxx} + \kappa^2 \hat{w}_{1,xx} = q^* - \kappa^2 w_{0,xx} \quad . \tag{51}$$

The general solution of D. E. (51), making use of symmetry around the origin, is

$$\hat{w}_1(x) = A_1 + A_3 \cos \kappa x + R_1 x^2 - R_2 \cos \frac{\pi x}{\ell}; \quad 0 \leq x \leq \ell, \tag{52}$$

where

$$R_1 = \frac{q^*}{2\kappa^2}; \qquad R_2 = \frac{f\kappa^2}{2[(\frac{\pi}{\ell})^2 - \kappa^2]} \quad . \tag{53}$$

Integrating D. E. (48.d) once, it follows that

$$-EA(\hat{\epsilon}_{2xx} - \alpha T) = \text{const.} = N^* \quad . \tag{54}$$

Utilizing B. C. (49).(e), it follows that

$$N^* = N \quad . \tag{55}$$

Making use of (54) and (55), D. E. (48.c) reduces to

$$\hat{w}_{2,xxxx} + \kappa^2 \hat{w}_{2,xx} = q^* \quad . \tag{56}$$

The general solution of (56) is

$$\hat{w}_2(x) = C_1 + C_2 x + C_3 \cos \kappa x + C_4 \sin \kappa x + R_1 x^2; \quad \ell \leq x \leq a \quad . \tag{57}$$

The constants in $\hat{w}_1(x)$ and $\hat{w}_2(x)$, A_1, A_3, C_1, C_2, C_3 and C_4, can be determined by substituting equations (52) and (57) into B. C.'s (49(f), (g), (h), (i), (ℓ), (m). The result may be written in the following form:

$$\begin{bmatrix} 1 & \cos \kappa\ell & -1 & -\ell & -\cos \kappa\ell & -\sin \kappa\ell \\ 0 & -\kappa \sin \kappa\ell & 0 & -1 & \kappa \sin \kappa\ell & -\kappa \cos \kappa\ell \\ 0 & -\kappa^2 \cos \kappa\ell & 0 & 0 & \kappa^2 \cos \kappa\ell & \kappa^2 \sin \kappa\ell \\ 0 & \kappa^3 \sin \kappa\ell & 0 & 0 & -\kappa^3 \sin \kappa\ell & \kappa^3 \cos \kappa\ell \\ 0 & 0 & 1 & a & \cos \kappa a & \sin \kappa a \\ 0 & 0 & 0 & 1 & -\kappa \sin \kappa a & \kappa \cos \kappa a \end{bmatrix} \begin{bmatrix} A_1 \\ A_3 \\ C_1 \\ C_2 \\ C_3 \\ C_4 \end{bmatrix} = \begin{bmatrix} -R_2 \\ 0 \\ (\frac{\pi}{\ell})^2 R_2 \\ 0 \\ -R_1 a^2 \\ -R_1 a \end{bmatrix} \quad 58)$$

However to solve for the unknown constants in equation (58), the value of a should be known for a given value of κ. This requires the use of one more B. C.; namely, T. C. (49)(p).

Substitution of (57) into (49)(p) gives

$$C_3 \kappa^2 \cos \kappa a + C_4 \kappa^2 \sin \kappa a - q^*/\kappa^2 = 0 \quad . \qquad 59)$$

Since the solution for a depends on C_3 and C_4, the process of determining the constants reduces to the solution of a set of non-linear algebraic equations. The solution may be obtained through an iterative scheme. Evaluating the constants for a given value of a and κ will define completely $\hat{w}_1(x)$ and $\hat{w}_2(x)$. Now one may proceed to evaluate the corresponding increase in temperature as follows:

Equation (50) may be rewritten as follows:

$$\hat{u}_{1,x} = (\frac{-N}{EA} + \alpha T) - (\frac{1}{2} \hat{w}_{1,x}^2 + w_{o,x} \hat{w}_{1,x}) \quad . \qquad 60)$$

Integrating once, noting B. C. (49)(a), it follows that

$$u_1(\ell) = (\frac{-N}{EA} + \alpha T)\ell - \int_0^\ell (\frac{1}{2} \hat{w}_{1,x}^2 + w_{o,x} \hat{w}_{1,x}) dx \quad . \qquad 61)$$

Similarly, (48)(d) gives

$$\hat{u}_{2,x} = \left(\frac{-N}{EA} + \alpha T\right) - \frac{1}{2}\hat{w}_{2,x}^2 \quad . \tag{62}$$

Integrating once, (62) becomes

$$\hat{u}_2(a) = \hat{u}_2(\ell) + \left(\frac{-N}{EA} + \alpha T\right)(a - \ell) - \int_{\ell}^{a} \frac{1}{2}\hat{w}_{2,x}^2 dx \quad . \tag{63}$$

Noting B. C. (49)(d), (63) becomes

$$\hat{u}_2(a) = \left(\frac{-N}{EA} + \alpha T\right)a - \int_0^{\ell} \left(\frac{1}{2}\hat{w}_{1,x}^2 + w_{0,x}\hat{w}_{1,x}\right)dx - \int_{\ell}^{a} \frac{1}{2}\hat{w}_{2,x}^2 \, dx \quad . \tag{64}$$

The general solution of D. E. (48)(f), noting (48)(g), is

$$\hat{u}_3(x) = D_1 e^{-\beta x} + D_2 e^{+\beta x} \quad , \tag{65}$$

where β is defined in (39).

Using B. C. (49)(q), (65) becomes

$$\hat{u}_3(x) = D_1 e^{-\beta x} \quad . \tag{66}$$

Substitution of (66) into B. C. (49)(k), it follows that

$$D_1 = \frac{-e^{+\beta a}}{\beta}\left(\frac{-N}{EA} + \alpha T\right) \quad , \tag{67}$$

and (66) becomes

$$\hat{u}_3(x) = \frac{-e^{-\beta(x-a)}}{\beta}\left(\frac{-N}{EA} + \alpha T\right) . \qquad 68)$$

Using B. C. (49)(j), it follows that

$$T = \left\{\frac{N}{EA} + \frac{\int_0^{\ell}(\frac{1}{2}\hat{w}_{1,x}^2 + w_{o,x}\hat{w}_{1,x})dx + \int_{\ell}^{a}\frac{1}{2}\hat{w}_{2,x}^2\,dx}{(a + \frac{1}{\beta})}\right\}/\alpha , \qquad 69)$$

which is the increase in temperature corresponding to the obtained equilibrium configuration of $\hat{w}_1(x)$ and $\hat{w}_2(x)$.

The numerical results of an example problem are presented in Figures 8 and 9 for the same track parameters of Case (A). The span of imperfection, 2ℓ, is taken to be 1.0 meter, while the imperfection amplitude, f, varies from 0.0 to 0.1 meter.

In Figure 8, the relation between the increase in temperature and the corresponding maximum deflection is presented. The bifurcation temperatures, although sharply reduced by increasing the imperfection amplitude, are still higher than those in Case (A) (for the same f/ℓ ratio); e.g., an f/ℓ ratio of 1/50 corresponds to a bifurcation temperature of 53°C in Case (A), Figure 3, while the corresponding value in Case (B) is 360°C, Figure 8. This observation is found to be valid for different imperfection spans. In this example problem the safe-temperature increase as well as the post-buckling response on the stable parts of the equilibrium branches is slightly affected by increasing the imperfection amplitude. The relation between the axial load in the lift-off region and the maximum deflection is shown in Figure 9. It should be noted that the bifurcation loads, although dropping at the same rate as the bifurcation temperatures, exceed the yield loads for the rails. However, buckling may still occur at lower temperatures by giving the track enough energy to reach the unstable part of the equilibrium branch.

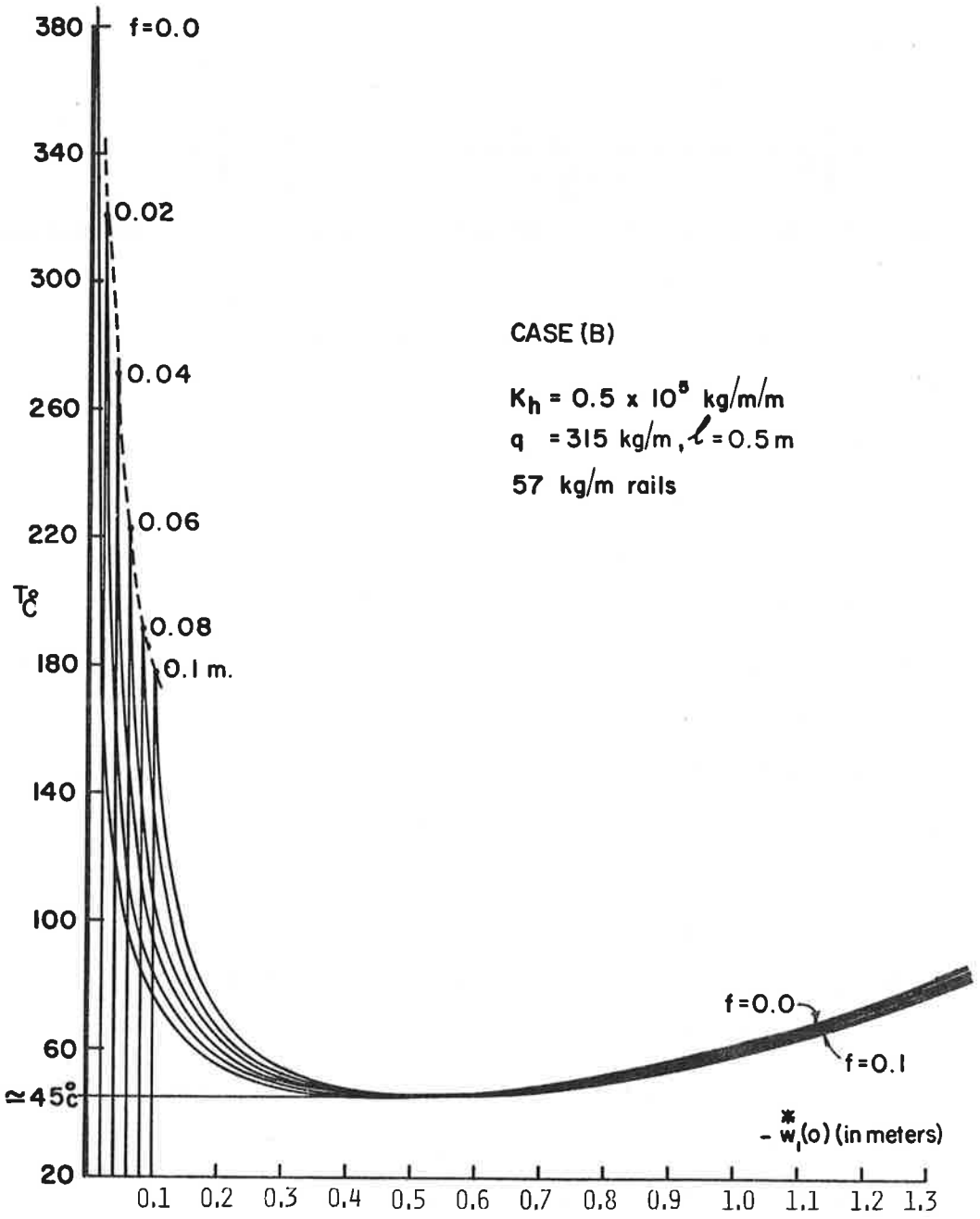

FIGURE 8. TEMPERATURE INCREASE VS. MAXIMUM DEFLECTION FOR CASE (B) (LIGHT TRACK)

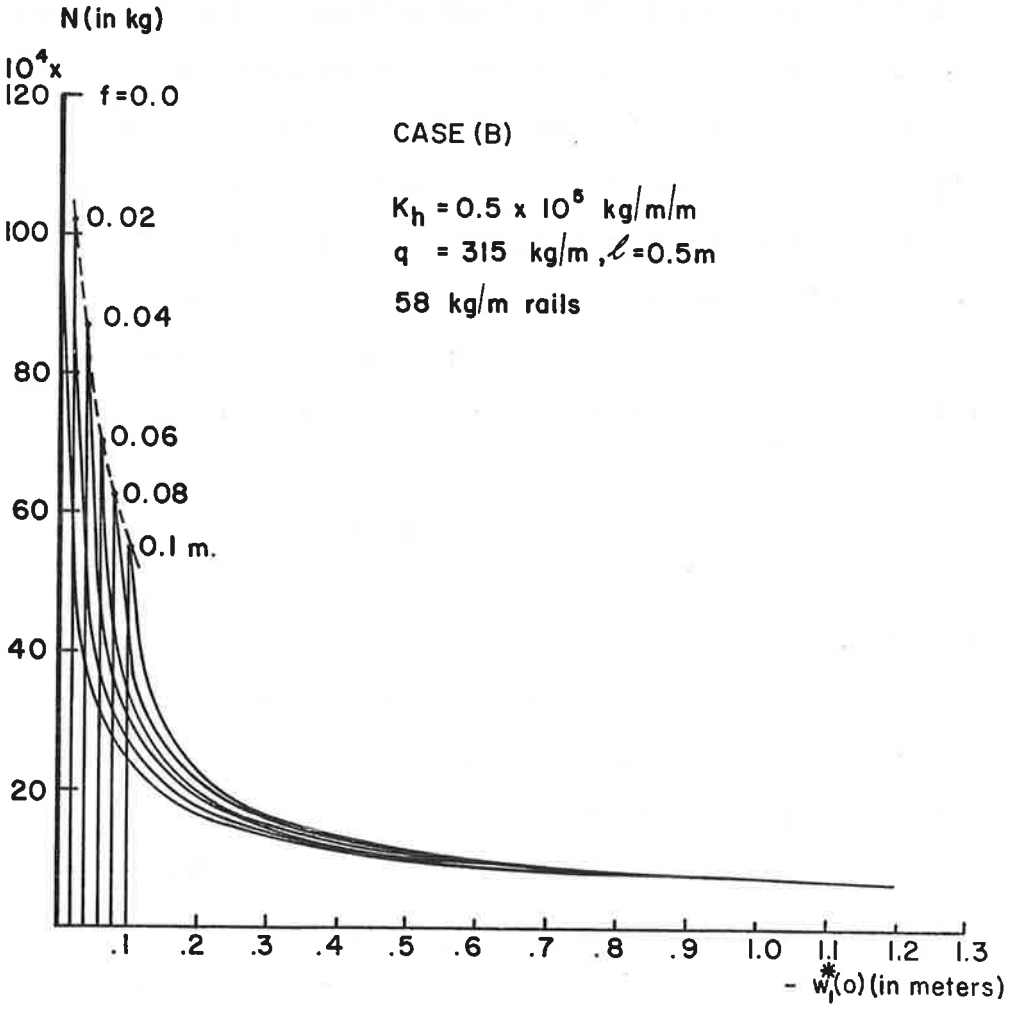

FIGURE 9. AXIAL LOAD IN BUCKLED REGION VS. MAXIMUM DEFLECTION FOR CASE (B) (LIGHT TRACK)

3. DISCUSSION OF RESULTS

In the preceding sections the example problems were solved for particular values of the imperfection span, 2ℓ, to show the effect of varying the imperfection amplitude on the bifurcation temperature as well as on the safe temperature increase.

Since the imperfection spans encountered in the field may vary from very short spans in the case of localized imperfection to very long spans in cases of slopes or shallow hills, it is important to examine the effect of varying the imperfection span on the safe temperature increase. Figure 10, shows the relation between the safe temperature increase, which is denoted by T_s, and the imperfection half span ℓ for positive imperfections.

The matching of the two solutions in Cases (A) and (B) occurs when the lift-off span coincides with the imperfection span. Noting that the formulation of the problem is in the Lagrange coordinate system, matching occurs when

$$\ell = \bar{a}$$

where $\bar{a}$ is the Euler coordinate of the separation point

and $$\bar{a} = a + \hat{u}_1(a)$$

However, for all practical purposes $\bar{a} \cong a$.

In Figure 10, it should be noted that compared to the straight state, positive imperfections give lower values for the safe temperature increase except on relatively short spans.

This finding may seem rather unusual, based on physical intuition, however, the fact that T_s is not a bifurcation temperature but rather a point of minima on a non-linear response curve may justify this behavior.

A similar set of graphs can be obtained for the concrete tie track, simply by using the corresponding track parameters in the analyses. The results will be similar except for a higher safe temperature increase.

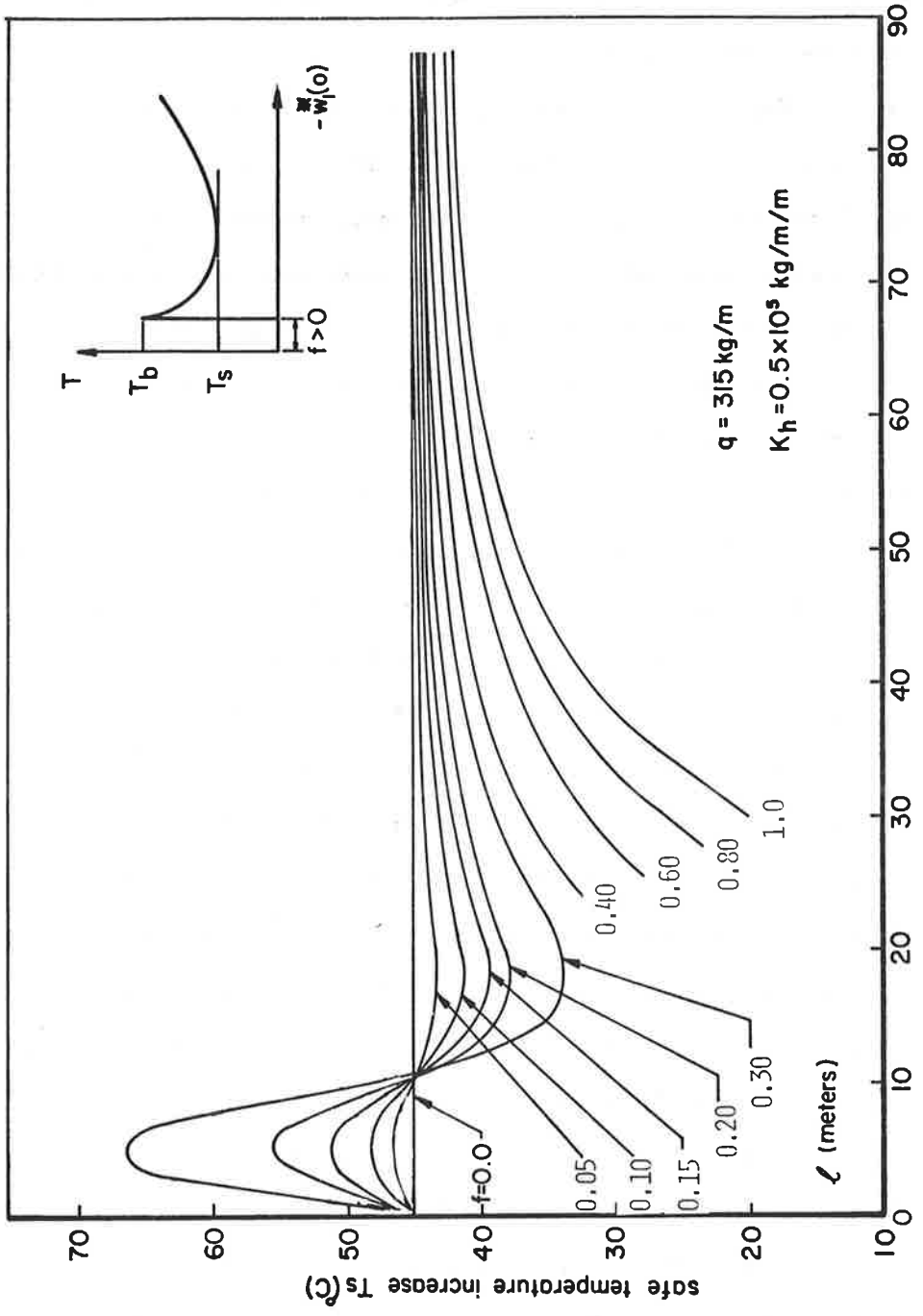

FIGURE 10. SAFE TEMPEARATURE INCREASE VS. HALF-SPAN OF IMPERFECTION FOR A LIGHT TRACK

4. CONCLUSIONS AND RECOMMENDATIONS

The analysis of the problem of vertical buckling of tracks with geometric imperfections shows that:

1) A perfectly straight track does not exhibit bifurcation points from the undeformed branch, while the imperfect track does.
2) Increasing the imperfection amplitudes reduces the bifurcation loads significantly. This is of some importance because if the imperfection is large enough, the bifurcation temperature may be as low as the safe temperature increase, and a very small disturbance may cause the track to buckle.
3) For the same f/ℓ ratio, the bifurcation temperature and the corresponding axial load are much higher in Case (B) than in Case (A).
4) By increasing the imperfection span, the safe temperature increase approaches that of a perfectly straight track.
5) The bifurcation temperature as well as the safe temperature increase are both increased by increasing the weight of the tracks.
6) The fact that the bifurcation loads may be higher than the yield loads of the rails does not mean that failure will occur only by yielding. If at lower temperature, that are higher than the safe temperature, the track is given enough energy to reach the state of unstable equilibrium it will snap through to the state of stable equilibrium. Such energy may be given either by the waves caused by the moving trains or by lifting the track during any maintenance process.

Since small vertical imperfections (which always exist in an actual track) strongly reduce the buckling temperature, it follows that the weight of the unit track and its flexural rigidity in the vertical plane (quantities which do not change significantly with time) are the dominant factors for vertical buckling.

5. REFERENCES

1. Kerr, A. D., "On the Stability of the Railroad Track in the Vertical Plane", Rail International, Feb., 1974, pp. 131-142.

2. Kerr, A. D., and El-Aini, Y. M., "On the Determination of Safe Buckling Temperature of a Railroad Track", DOT Report, Princeton University, Dec. 1974.

3. El-Aini, Y. M., "On the Vertical Buckling of a Railroad Track", Ph.D. Thesis, New York University, May 1974.

4. Kerr, A. D., "A Model Study for Vertical Track Buckling", High Speed Ground Transp. J., Vol. 7, No. 3, 1973, pp. 351-368.

5. Kerr, A. D., "On the Derivation of Well-Posed Boundary Value Problems in Structual Mechanics", Int. J. Solids Structures, Vol. 12, 1976, pp. 1-11.

6. Novozhilov, V. V., "Theory of Elasticity" (In Russian), Sudpromgiz, 1958. English translation available from OTS, U.S. Dept. of Commerce, as OTS 61-11401.

7. Elsgolc, L. E., Calculus of Variations, Pergamon Press, LTD., 1962.

8. Hay, W. W., Railroad Engineering, John Wiley & Sons, Inc., NY, 1953.

9. "Track Building: How SP is doing it on long cut-off line", Railway Track and Structures, July 1967, Vol. 63, No. 7, pp. 20-23.

APPENDIX

REPORT OF INVENTIONS

After a diligent review of the work performed under this contract, no innovation, discovery, or invention was made. The work involved developing and improving the predictive capability of vertical track buckling analyses.